

ANOs 3–7 in the anoctamin/Tmem16 Cl[−] channel family are intracellular proteins

Charity Duran,¹ Zhiqiang Qu,¹ Adeboye O. Osunkoya,² Yuanyuan Cui,¹ and H. Criss Hartzell¹

¹Department of Cell Biology and Center for Neurodegenerative Disease, and ²Department of Pathology, Emory University School of Medicine, Atlanta, Georgia

Submitted 3 May 2011; accepted in final form 8 November 2011

Duran C, Qu Z, Osunkoya AO, Cui Y, Hartzell HC. ANOs 3–7 in the anoctamin/Tmem16 Cl[−] channel family are intracellular proteins. *Am J Physiol Cell Physiol* 302: C482–C493, 2012. First published November 9, 2011; doi:10.1152/ajpcell.00140.2011.—Ca²⁺-activated Cl[−] channels (CaCCs) participate in numerous physiological functions such as neuronal excitability, sensory transduction, and transepithelial fluid transport. Recently, it was shown that heterologously expressed anoctamins ANO1 and ANO2 generate currents that resemble native CaCCs. The anoctamin family (also called Tmem16) consists of 10 members, but it is not known whether all members of the family are CaCCs. Expression of ANOs 3–7 in HEK293 cells did not generate Cl[−] currents activated by intracellular Ca²⁺, as determined by whole cell patch clamp electrophysiology. With the use of confocal imaging, only ANO1 and ANO2 traffic to the plasma membrane when expressed heterologously. Furthermore, endogenously expressed ANO7 in the human prostate is predominantly intracellular. We took a chimeric approach to identify regions critical for channel trafficking and function. However, none of the chimeras of ANO1 and ANO5/7 that we made trafficked to the plasma membrane. Our results suggest that intracellular anoctamins may be endoplasmic reticulum proteins, although it remains unknown whether these family members are CaCCs. Determining the role of anoctamin family members in ion transport will be critical to understanding their functions in physiology and disease.

anion transport; chloride channels; calcium-activated chloride channels

Ca²⁺-ACTIVATED Cl[−] channels (CaCCs) play important roles in physiological processes including sensory transduction, epithelial secretion, and smooth muscle contraction (9). Recently, three groups independently identified a gene encoding for a transmembrane protein (anoctamin 1, ANO1, TMEM16A) that closely recapitulates the properties of endogenous CaCCs (4, 35, 42). ANO1 is highly expressed in epithelial tissues, where it plays an important role in Ca²⁺-dependent Cl[−] secretion (7, 14, 18, 25, 26, 30). ANO1 can be activated both by intracellular Ca²⁺ and by activation of G protein-coupled receptors that raise intracellular Ca²⁺ (35, 42). ANO2 has also been shown to be a CaCC and mediates Ca²⁺-activated Cl[−] currents in olfactory sensory neurons and photoreceptor synapses (28, 29, 32, 37, 38).

The anoctamin family consists of 10 members, all of which are predicted to have eight transmembrane domains with cytosolic NH₂- and COOH-termini. With the possible exceptions of ANO8 and ANO10, anoctamins are predicted to have a reentrant loop between transmembrane domains 5 and 6 that has been suggested to participate in the ion selectivity filter (6,

11, 20, 42). While the predicted structural homology between family members is conserved, evolutionary analysis suggests that anoctamins have evolved distinctive functional properties (20). Furthermore, the diversity of endogenous CaCCs in various tissues indicates that CaCCs may be mediated by more than one protein molecule. Although other anoctamin family members are, in fact, expressed in epithelial tissues, it is not known whether these function as CaCCs. We find that unlike ANO1 and ANO2, ANOs 3–7 do not generate Cl[−] currents activated by intracellular Ca²⁺ when expressed in human embryonic kidney 293 (HEK293) cells, as determined by whole cell patch clamp electrophysiology. Localization studies demonstrate that several anoctamin family members do not traffic to the plasma membrane in HEK293 cells and may reside in the endoplasmic reticulum (ER). We took a chimeric approach to determine which regions are important for anoctamin trafficking and function, with an emphasis on ANOs 5 and 7. We chose to focus on ANO5 and ANO7 because of their roles in disease. ANO5 was originally identified as the gene responsible for the rare bone disease gnathodiaphyseal dysplasia (GDD1) (21, 39) and has more recently been linked to several limb girdle muscular dystrophies (2, 12, 17). ANO7 is implicated in prostate cancer, as it was discovered in a search for genes whose expression patterns mimicked those of known prostate cancer genes (15).

MATERIALS AND METHODS

Cell culture and transfection. HEK293 and COS-7 cells were cultured in DMEM supplemented with 10% fetal bovine serum and 0.5% penicillin-streptomycin at 37°C. Chinese hamster ovary (CHO) and Fischer rat thyroid (FRT) cells were cultured in Ham's F-12 medium supplemented with 2 mM L-glutamine, 10% fetal bovine serum, and 0.5% penicillin-streptomycin at 37°C. The 22Rv1-ANO7 cell line (generously provided by Ira Pastan, NIH) was cultured in RPMI 1640 containing 10% FBS, 1 mmol/l pyruvate, 2 mmol/l glutamine, and 100 µg/ml penicillin, and 100 µg/ml streptomycin. For electrophysiology, low-passage HEK293 cells were transfected using Fugene 6 with 1 µg of green fluorescent protein (GFP)-tagged anoctamin constructs. For cotransfections, 0.5 µg of each construct were used. Transfected cells were then plated at low density and used for electrophysiology 24–48 h after transfection. Cells expressing the GFP-fusion proteins were patched. For immunofluorescence, all cell types were transfected with 1 µg of DNA using lipofectamine 2000 (Invitrogen). For colocalization with the mCherry-17 ER marker (3, 31) (generously provided by Catherine Hartzell, Stanford University), cells were transfected with 1 µg of the 17-mCherry construct in addition to 1 µg of the ANO7-myc construct.

Electrophysiology. Recordings were performed using the whole cell patch clamp configuration. Patch pipettes had resistances of 2–4 MΩ. Data were acquired by an Axopatch 200A amplifier controlled by Clampex 8.2 via a Digidata 1322A data acquisition system (Molecular Devices). Voltage ramps of 200 ms from −100 to +100 mV

Address for reprint requests and other correspondence: H. C. Hartzell, 615 Michael St., 535 Whitehead Bldg., Atlanta, GA 30322-3030 (e-mail: criss.hartzell@emory.edu).

were applied at 10-s intervals, followed by a voltage-step protocol from -100 to $+100$ mV in 20-mV intervals applied every 10 s. Data were analyzed using ClampFit 8.2 software (Molecular Devices).

Solutions. The high Ca^{2+} ($\sim 24 \mu\text{M}$ free Ca^{2+}) intracellular pipette solution contained (in mM) 146 CsCl, 2 MgCl_2 , 5 Ca-EGTA , 10 sucrose, and 8 HEPES, pH 7.3 with NMDG. Different free $[\text{Ca}^{2+}]$ solutions were made by mixing the high Ca^{2+} solution with a Ca^{2+} -free solution containing 5 mM EGTA as described previously (16). The extracellular solution contained (in mM) 140 NaCl , 5 KCl , 2 CaCl_2 , 1 MgCl_2 , 15 glucose, and 10 HEPES, pH 7.4 with NaOH. Osmolarity was adjusted with sucrose to 303 mosM for all solutions.

Anoctamin constructs. mANO1 tagged with enhanced GFP (EGFP) on the COOH-terminus was generously provided by Prof. Uhtaek Oh, Seoul National University. hANO7 tagged with myc on the COOH-terminus was provided by Ira Pastan, NIH, and was tagged on the COOH-terminus with EGFP or mCherry by subcloning into pEGFP-N1 or pmCherry. The hANO5 construct was purchased from Open Biosystems (I.M.A.G.E. ID: 100061756) and tagged with EGFP on the COOH-terminus by subcloning into pEGFP-N1. All other ANO constructs were cloned from mouse tissues using RT-PCR and subsequently subcloned into pEGFP-N1 (mANO2, NM_153589.2; mANO4, NM_178773.4; mANO6, NM_175344.3; mANO10, NM_133979.2).

Generation of chimeric constructs. Chimeras were constructed using overlapping PCR (13). After PCR, the products were digested and subsequently ligated into the pEGFP vector.

Immunoblot. Cells in culture were homogenized in lysis buffer containing 1% Triton X-100, 1 mM EDTA, 50 mM Tris-HCl (pH 7.4), and protease inhibitor cocktail III (Calbiochem) plus 10 μM phenylmethylsulfonyl chloride. Samples were diluted in SDS Laemmli buffer, and aliquots were run on 7.5% reducing SDS-PAGE and transferred to nitrocellulose. ANO7 antibody was used at a 1:1,000 dilution and detected by enhanced chemiluminescence (Super Signal, Thermo Scientific).

Immunofluorescence. Cells were plated on poly-D-lysine-coated coverslips. One to two days after transfection, cells were fixed for 20 min in 4% paraformaldehyde. Cells were then washed in PBS, incubated in a PBS blocking solution containing saponin (0.025%) and either BSA (3%) or 1% cold fish water gelatin for 30 min at room temperature, and subsequently incubated with primary antibodies (1:1,000) overnight at 4°C. Primary antibodies were used against the following antigens: hANO7 (generously provided by Dr. Ira Pastan, NIH, directed against amino acids 875–933, IPES...QLQQ), mANO1 (amino acids 878–960 MSDF...GDAL, SDIX custom Genomic Antibody, Newark DE), mouse anti-myc (1:1,000, Invitrogen), rabbit anti-calnexin (1:300, Enzo Life Sciences), mouse anti-calnexin (1:50 BD Biosciences), sheep anti-TGN46 (1:150, AbD Serotec), KDEL receptor (1:200, Stressgen), and mouse anti-EEAI (1:100 BD Biosciences). For determining ANO7 antibody specificity, antibody was preincubated with immunizing peptide for 1 h at room temperature. The cells were then washed and incubated with a mixture of Alexa 488- or Alexa 568-conjugated (1:1,000) secondary antibodies for 1 h at 4°C, and either rhodamine-conjugated wheat germ agglutinin (2 $\mu\text{g}/\text{ml}$) (WGA, Invitrogen) for 10 min at room temperature, or Alexa 633-conjugated phalloidin (1:1,000, Invitrogen) for 1 h at 4°C. Coverslips were mounted on glass slides using ProLong Gold (Invitrogen).

Human prostate tissue. Sections of frozen tissue from radical prostatectomy specimens were obtained from the Prostate Tissue Satellite Bank of the Human Tissue Procurement Service of Emory University. Formalin-fixed paraffin-embedded tissue from the same patients were also obtained. All the sections utilized for this study were from areas composed exclusively of benign prostatic tissue. Frozen sections (20 μm thick) were fixed for 1 h in 4% paraformaldehyde in 0.1 M phosphate buffer, pH 7.3, rinsed 3× in PBS, and blocked with 1% cold fish water gelatin in PBS for 1 h. Paraffin-embedded sections were deparaffinized with two washes in xylene for 5 min followed by rehydration with serial dilutions of ethanol.

Sections were heated in a water bath (20 min at 85°C) in citrate buffer for antigen retrieval. Both frozen and paraffin-embedded sections were incubated with primary antibodies overnight at 4°C. Antibodies were used against the following antigens: anti-alpha Na^+-K^+ -ATPase, (a6F-c, 1:100, Developmental Studies Hybridoma Banks, University of Iowa), calnexin (1:50, BD Biosciences), rabbit anti-ATP12A (1:50, Sigma), and aquaporin-3 (Santa Cruz Biotechnology). Use of human tissue was approved by the Emory University Institutional Review Board. Tissue samples were deidentified and impossible for us to trace back to the patient's identity.

Bioinformatic analysis. Protein and nucleotide alignments and pairwise comparisons were performed using Lasergene 7.0 and CLC Main Workbench 5.6. Transmembrane helices were predicted using MemBrain, which integrates sequence representation by multiple sequence alignment matrix, optimized evidence-theoretic K-nearest neighbor prediction, fusion of multiple prediction window sizes, and classification by dynamic threshold (36). Type-II divergence was determined using DIVERGE 2.0 (<http://xgu.zool.iastate.edu/software.html>). GENBANK accession numbers of sequences used for the DIVERGE analysis were the following: Ano1: NP_001101034, NP_848757, XP_610636, NP_060513, XP_854489, XP_002194623, XP_421072, NP_001128709, NP_001123799, NP_001155062; Ano2: XP_508944, NP_065106, XP_001495378, XP_001066367, NP_70581, XP_001118212, XP_590066, XP_001368614, XP_002188249; Ano5: NP_998764, XP_001918124, NP_808362, NP_001086810, NP_001073452; Ano7: NP_996914, NP_001004071, NP_001001891, XP_684890, XP_001377095.

RESULTS

Expression of ANOs 3–7 do not generate Ca^{2+} -activated Cl^- currents in HEK293 cells. We performed whole cell recordings on HEK293 cells transiently transfected with anoctamin constructs (ANO 1–7) (Fig. 1). Cells transfected with GFP alone had negligible Cl^- currents ($<100 \text{ pA}$ in amplitude at $+100$ mV). Expression of GFP-tagged ANO1 produced currents that were Ca^{2+} dependent. ANO1 currents were outwardly rectifying at intracellular $[\text{Ca}^{2+}] < 1 \mu\text{M}$ and nearly linear at higher $[\text{Ca}^{2+}]$ (Fig. 1, A and B). ANO2 currents were also Ca^{2+} dependent but activated more quickly and exhibited more pronounced outward rectification at high Ca^{2+} (Fig. 1, A and B). The mean peak amplitudes of currents at $+100$ mV with 24 μM intracellular Ca^{2+} were $13 \pm 1.8 \text{ nA}$ for ANO1 and $4 \pm 1.2 \text{ nA}$ for ANO2. In contrast, cells transfected with ANOs 3–7 had currents that were the same as GFP controls (Fig. 1C). ANO7 has been reported to support a very small iodide flux in transfected FRT cells (34), but in our hands expression of ANO7 in FRT cells did not yield significant Ca^{2+} -activated currents at $+100$ mV, as measured by whole cell patch clamp electrophysiology ($31 \pm 12 \text{ pA}$, $n = 3$).

Because many ion channels are heteromeric, we tested whether the absence of currents could be explained by the absence of another subunit. We coexpressed ANO7, which is not detected in HEK cells by RT-PCR or Western blot, with ANO1, ANO2, ANO4, ANO5, ANO6, and ANO10. Combinations that included ANO1 were tested at 180 nM Ca^{2+} to avoid maximal current activation, whereas combinations with other ANOs were tested at 24 μM Ca^{2+} . None of these anoctamin combinations generated Cl^- currents, with the exception of coexpression of ANO7 with ANO1 or ANO2 (Fig. 1D). mANO1+hANO7 produced currents of similar amplitude as mANO1 alone at the same $[\text{Ca}^{2+}]$ ($\sim 180 \text{ nM}$). Similarly, mANO2+hANO7 produced currents of similar amplitude to mANO2 alone at the same $[\text{Ca}^{2+}]$ ($\sim 24 \mu\text{M}$).

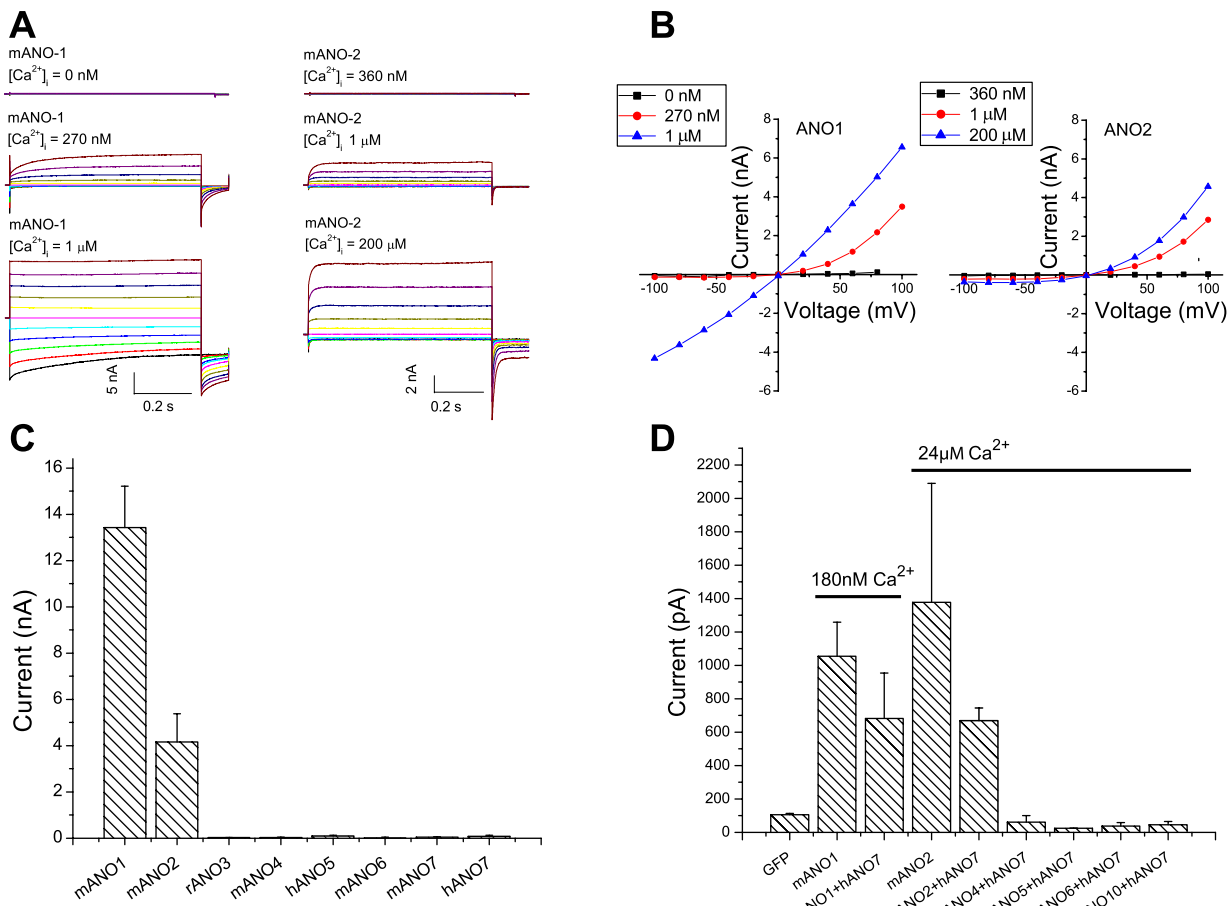


Fig. 1. Anoctamin whole cell current response to intracellular [Ca²⁺]. *A*: representative current traces for mANO1 and mANO2 at different intracellular [Ca²⁺]. Different free [Ca²⁺] solutions were made by mixing the high Ca²⁺ solution with a Ca²⁺-free solution containing 5 mM EGTA (16). *B*: mean current-voltage (*I*-*V*) relationship for ANO1 and ANO2 in response to different intracellular [Ca²⁺]. *C*: current amplitude at +100 mV of mANO1, mANO2, rANO3, mANO4, mANO7, hANO5, mANO6, and hANO7 as indicated with an intracellular solution containing 5 mM Ca-EGTA (~24 μM free Ca²⁺). *N* = 3–7 for each condition. *D*: current amplitude at +100 mV of hANO7 coexpressed with various ANOs as indicated in response to ~24 μM intracellular [Ca²⁺] or ~180 nM [Ca²⁺] for coexpression with ANO1. For transfection with individual ANO constructs, 1 μg DNA was used; cotransfections were performed using 0.5 μg of each ANO construct.

Plasma membrane trafficking of ANOs in various cell lines. ANO constructs with a COOH-terminal EGFP tag were overexpressed in HEK293, CHO, and COS-7 cells and analyzed using confocal microscopy (Fig. 2). Multiple cell lines were used in the event that HEK cells lacked an essential subunit or chaperone for proper trafficking. These cell lines originate from different species and tissues, and therefore provide a different proteomic background for favorable expression and trafficking. Similar results were obtained with all cell lines tested. ANO1 is clearly localized to the plasma membrane (Fig. 2A). In contrast, EGFP-tagged ANOs 3, 4, 5, 6, 7, and 10 are localized intracellularly (Fig. 2B). The intracellular localization of ANOs 3, 4, 5, 6, 7, and 10 is consistent with electrophysiology data, which shows that these ANOs do not produce Ca²⁺-activated Cl[−] currents when expressed in HEK293 cells.

To test whether the intracellular localization of ANO7 was possibly caused by the EGFP tag, we examined the localization of a myc-tagged construct. The myc tag is considerably shorter than the 238 amino acid EGFP tag and may be less likely to interfere with protein folding or trafficking. The localization of ANO7-myc was also intracellular like ANO7-EGFP (Fig. 2C). In Fig. 2C, the difference in localization between ANO1 and

ANO7 is shown clearly where ANO7-myc was coexpressed with ANO1-EGFP; ANO1 is localized to the plasma membrane, whereas ANO7 is intracellular. We observe a similar subcellular distribution of ANO1 and ANO7 when expressed in several cell lines, including HeLa and CHO cells.

Subcellular localization of anoctamins. In cells transfected with fluorescently tagged ANOs 3, 4, 5, 6, 7, and 10, a reticular pattern characteristic of ER is observed (Fig. 2B). Colocalization of ANO7 with mCherry-17, an ER marker, supports the conclusion that most of ANO7 is localized in the ER (Fig. 3A). Colabeling of cells for ANO7 and calnexin (CNX), another ER marker, reveal that while a portion of ANO7 colocalizes with CNX, some ANO7 is localized in a compartment adjacent to the CNX. These data indicate that some ANO7 is localized to an ER subdomain distinct from that of calnexin. ANO7 does not colocalize with other markers, including the KDEL receptor (cis-golgi), EEA1 (endosomes), or TGN46 (trans-golgi) (Fig. 3B). While we cannot rule out potential artifacts of overexpression in a heterologous system, these results suggest that intracellular anoctamins may be ER proteins.

Because the localization of heterologously expressed proteins might be abnormal for a variety of reasons, we examined the endogenous expression of ANO7 in the prostate using an

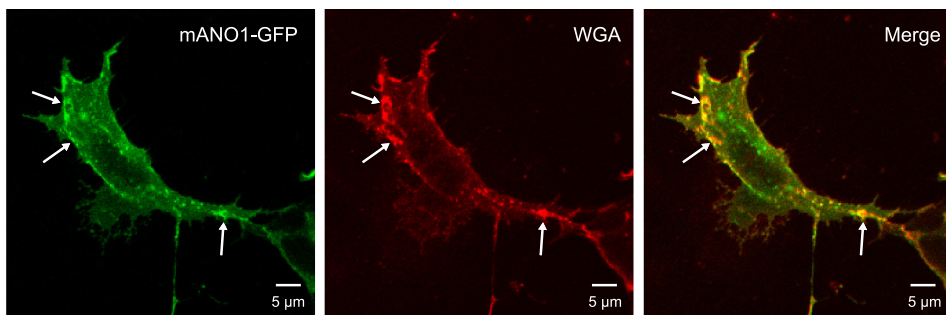
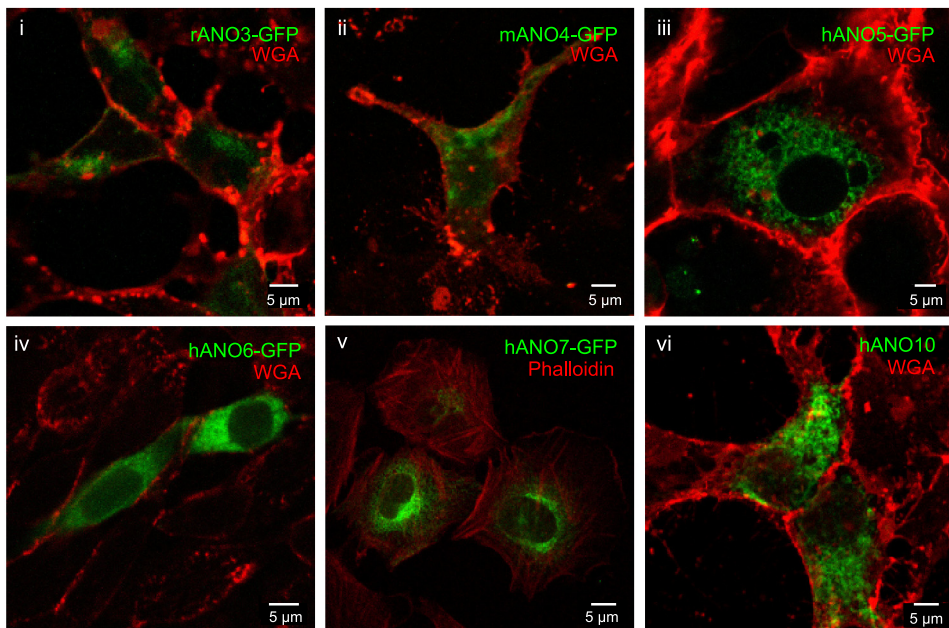
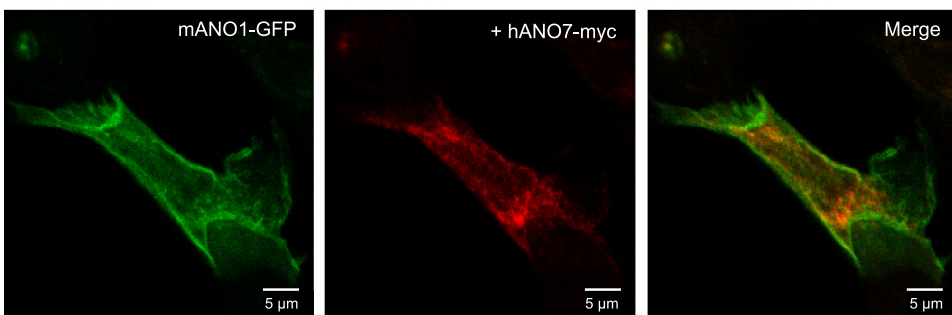
A**B**

Fig. 2. Immunofluorescence confocal microscopy of various cell types expressing ANOs 1, 3, 4, 5, 6, 7, and 10. *A*: HEK293 cells transiently transfected with green fluorescent protein (GFP)-tagged mANO1 alone. Arrows indicate colocalization of ANO1 with the membrane marker wheat germ agglutinin (WGA). *B*: various cell lines transiently transfected with GFP-tagged ANO constructs. Different cell types are shown for illustration, but these results are typical of all cell lines tested. *i, ii, vi*: HEK293 cells; *iii, v*: COS-7 cells; *vi*: CHO cells. Cells in *B, v* were counterstained with phalloidin for actin; all other cells were counterstained with a plasma membrane marker WGA. *C*: GFP-tagged mANO1 (green) coexpressed with myc-tagged hANO7 (red) in HEK293 cell.

C

antibody against the COOH-terminus of the long form of ANO7 (5, 6). The specificity of the antibody for the long form of ANO7 was confirmed by both immunoblot and immunofluorescence (Fig. 4). The antibody recognizes a 133-kDa band in HEK cells transfected with GFP-tagged ANO7 and a 106-kDa band corresponding to nontagged ANO7 in a stable cell line 22Rv1-ANO7 (Fig. 4A). No signal is detected in nontrans-

fected HEK293 cells or in 22Rv1 cells stably transfected with the empty vector. Furthermore, preincubation of the antibody with immunizing peptide abolishes the ANO7 signal (Fig. 4B). The antibody is also suitable for immunofluorescent staining, as antibody staining colocalizes with myc-tagged ANO7 (Fig. 4C). The staining can be abolished upon preincubation with the immunizing peptide.

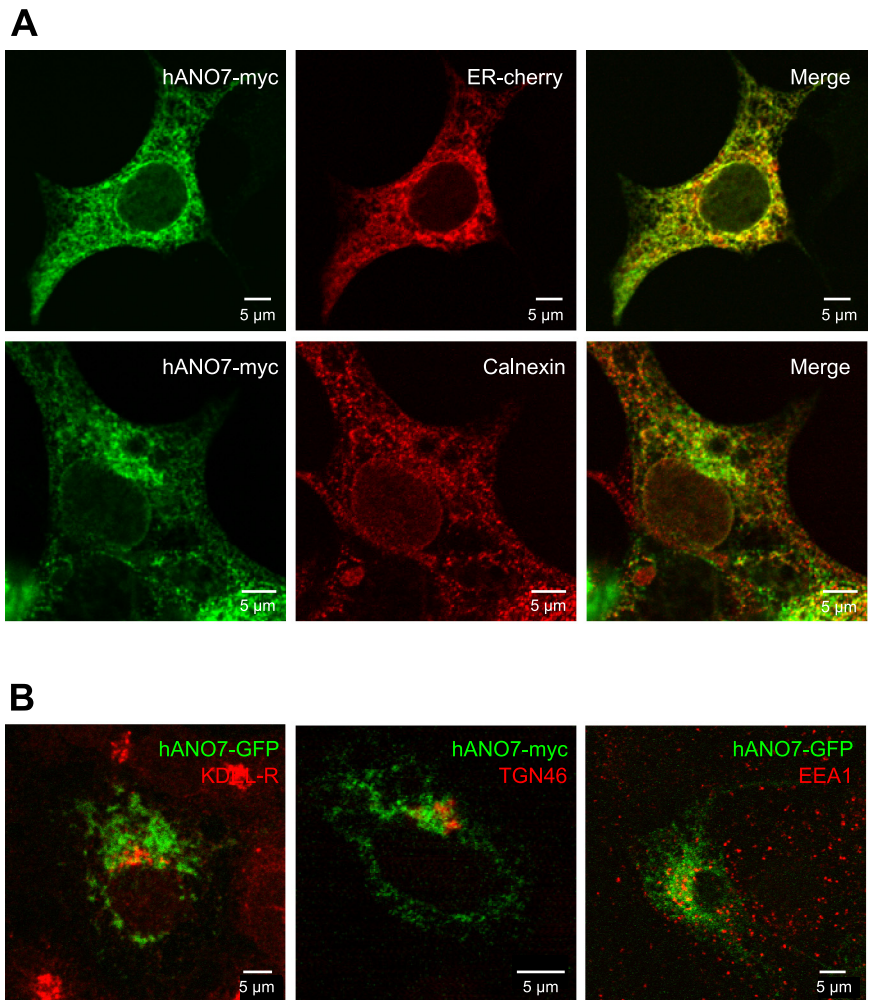


Fig. 3. Subcellular localization of ANO7. *A*: ANO7-myc colocalizes with endoplasmic reticulum (ER) marker mCherry-17, and partially colocalizes with the ER protein calnexin (CNX) in HEK293 cells. *B*: ANO7 does not colocalize with markers for KDEL Receptor (cis-golgi), TGN46 (trans-golgi), or EEA1 (endosomes) when expressed in HEK293 cells.

Localization of endogenous ANO7 in human prostate. Staining of human prostate tissue with the ANO7 antibody revealed that ANO7 was highly expressed in the prostatic epithelium when examined at low power (Fig. 5). At higher power, a significant portion of endogenous ANO7 appeared to be localized intracellularly. Basolateral membrane markers aquaporin 3 and Na⁺-K⁺-ATPase are clearly confined to the basolateral plasma membrane. In contrast, ANO7 appears to be localized intracellularly at the apical end of the cell. Much of the ANO7 staining is punctate, and there is no clearly defined apical staining (Fig. 5). We have tried to no avail to find a good apical plasma membrane marker, but none of the antibodies that we have tried (anti-aquaporin 3, anti-Na⁺-K⁺-ATPase, anti-H⁺-K⁺-ATPase) were localized apically (Fig. 5). As in HEK cells, ANO7 staining overlaps with that of calnexin, but the two proteins do not precisely colocalize.

Sequence homology across ANOs. There are 10 members of the anoctamin family. However, ANO1 and ANO2 comprise a distinct branch of the family tree. Protein sequence conservation analysis reveals that ANO1 displays the highest degree of conservation (~57% identical) with ANO2, the only other anoctamin shown clearly to be a CaCC. The percent identity between ANO1 and other anoctamin family members is lower, with ANO5 and ANO7 being ~30% identical to ANO1. If one includes structurally similar amino acids, ANO1 is 51% similar

to ANO7 and 59% similar to ANO5. Although anoctamins have a similar predicted membrane topology and display sequence conservation in TMDs, it is not clear whether all anoctamins are associated with Cl⁻ currents.

Evolutionary analysis using DIVERGE suggests that anoctamins may have diverse physiological functions. The regions exhibiting the highest functional divergence are the NH₂-terminus and the hydrophilic loops between transmembrane domains (Fig. 6). However, divergent amino acids are scattered throughout the protein and clustering provides little clue to identifying key amino acids that could account for differences in trafficking or function of the proteins. We therefore took a chimeric approach to identify regions between ANO1 and ANO5 or ANO7 critical for channel trafficking and function.

Chimeras between ANO1 and ANO5 or ANO7 do not generate Ca²⁺-activated Cl currents. Because protein NH₂- and COOH-termini frequently contain targeting signals important for protein trafficking and were identified as being different among ANO1 or 2 and ANO5 or 7 in the DIVERGE analysis, we generated chimeras containing either NH₂- or COOH-terminal sequences from ANO1. Functionality and localization of chimeras between ANO1 and ANO5 or ANO7 were analyzed using whole cell patch clamp electrophysiology and confocal microscopy. Replacement of the NH₂- or COOH-terminus of ANO7 with the corresponding

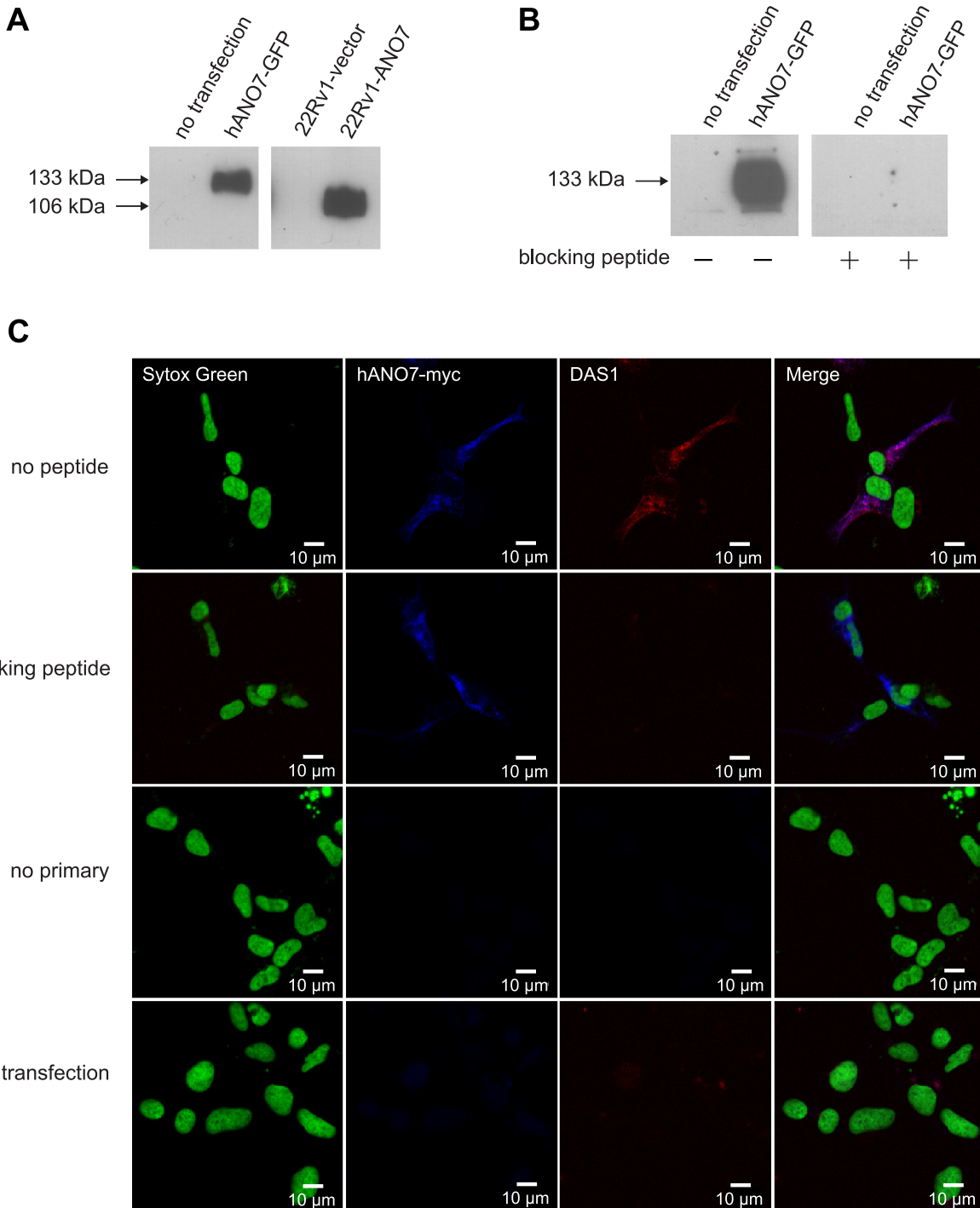


Fig. 4. Characterization of ANO7 antibody specificity. *A*: ANO7 antibody recognizes GFP-tagged ANO7 protein in transfected HEK293 cells and nontagged ANO7 in a stably transfected cell line 22Rv1-ANO7. No signal is detected in nontransfected HEK293 cells or 22Rv1 cells stably transfected with the empty vector. *B*: immunoblot showing that preincubation of ANO7 antibody with the immunizing peptide abolishes ANO7 staining in HEK293 cells transfected with GFP-tagged hANO7. *C*: ANO7 antibody (DAS1) staining in transfected HEK293 cells demonstrates that it colocalizes with myc-tagged ANO7. The staining is abolished upon preincubation of the antibody with immunizing peptide.

sequences from ANO1 (Fig. 7, chimeras 7–2 and 7–3, respectively) did not produce currents and were not trafficked to the plasma membrane. A chimera composed of ANO7 with an ANO1 NH₂-terminus and first transmembrane domain (chimera 7–4) was not trafficked to the plasma membrane. The inverse chimera composed of ANO1

with an ANO7 NH₂-terminus and first transmembrane domain (chimera 7–5) also was retained intracellularly. These data suggest that there are multiple trafficking signals in ANO7 that are involved in preventing trafficking to the plasma membrane. Analogous results were obtained with ANO1-ANO5 chimeras (Fig. 8). An ANO5 chimera con-

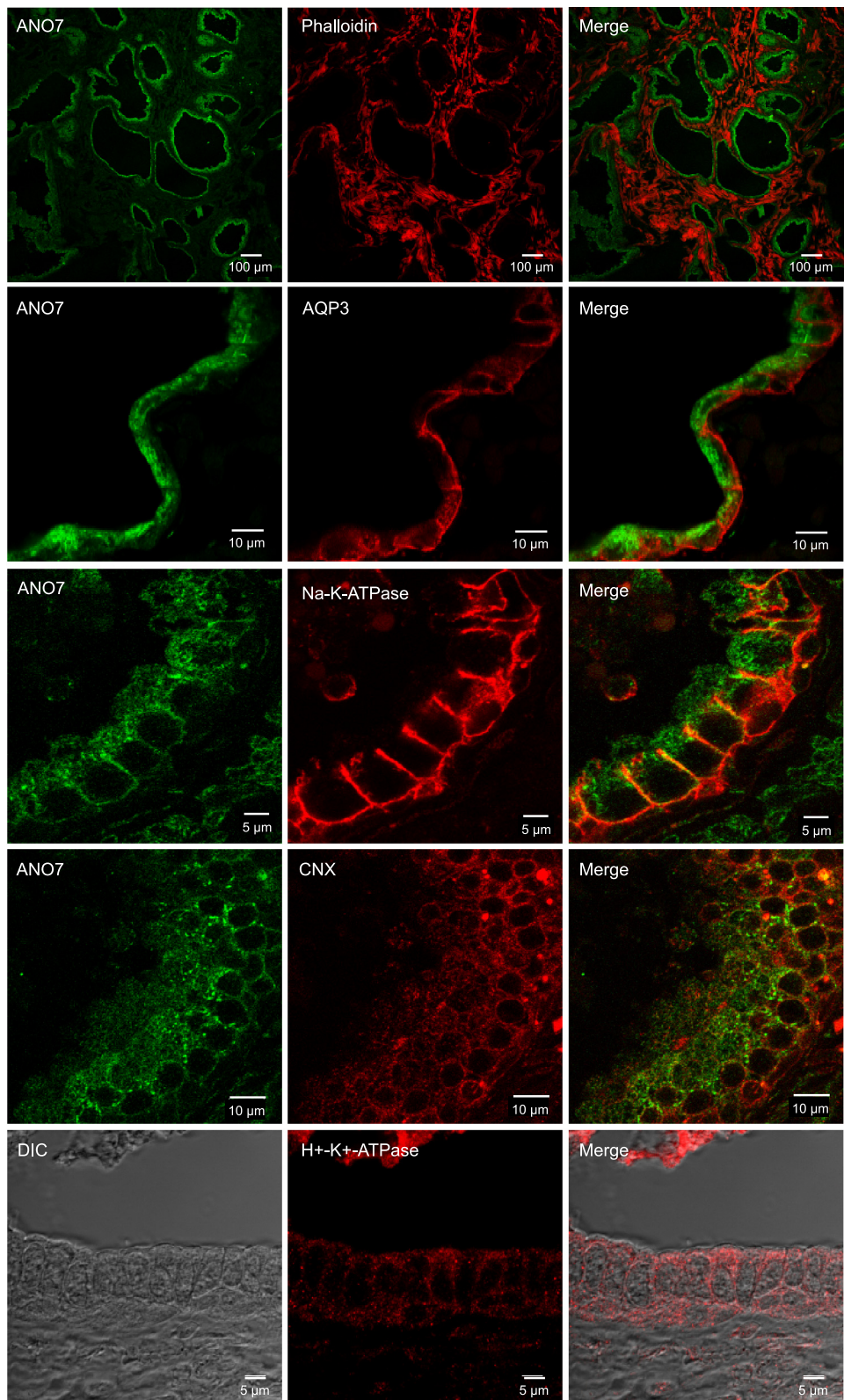


Fig. 5. Immunofluorescence confocal microscopy of human prostate expressing endogenous ANO7. Endogenous ANO7 (green) in prostate gland epithelium with various counterstains: phalloidin, aquaporin-3, Na^+/K^+ -ATPase, CNX, and H^+/K^+ -ATPase.

taining the ANO1 NH₂-terminus plus the first two transmembrane domains and first intracellular loop (chimera 5–2) was localized intracellularly and did not generate current (Fig. 8).

One possible explanation for the absence of currents generated by ANO5 and ANO7 is that these channels are not activated by Ca^{2+} but are activated by other mechanisms. We have found that the sequence ₄₄₄EEEEEAVK₄₅₂ in the

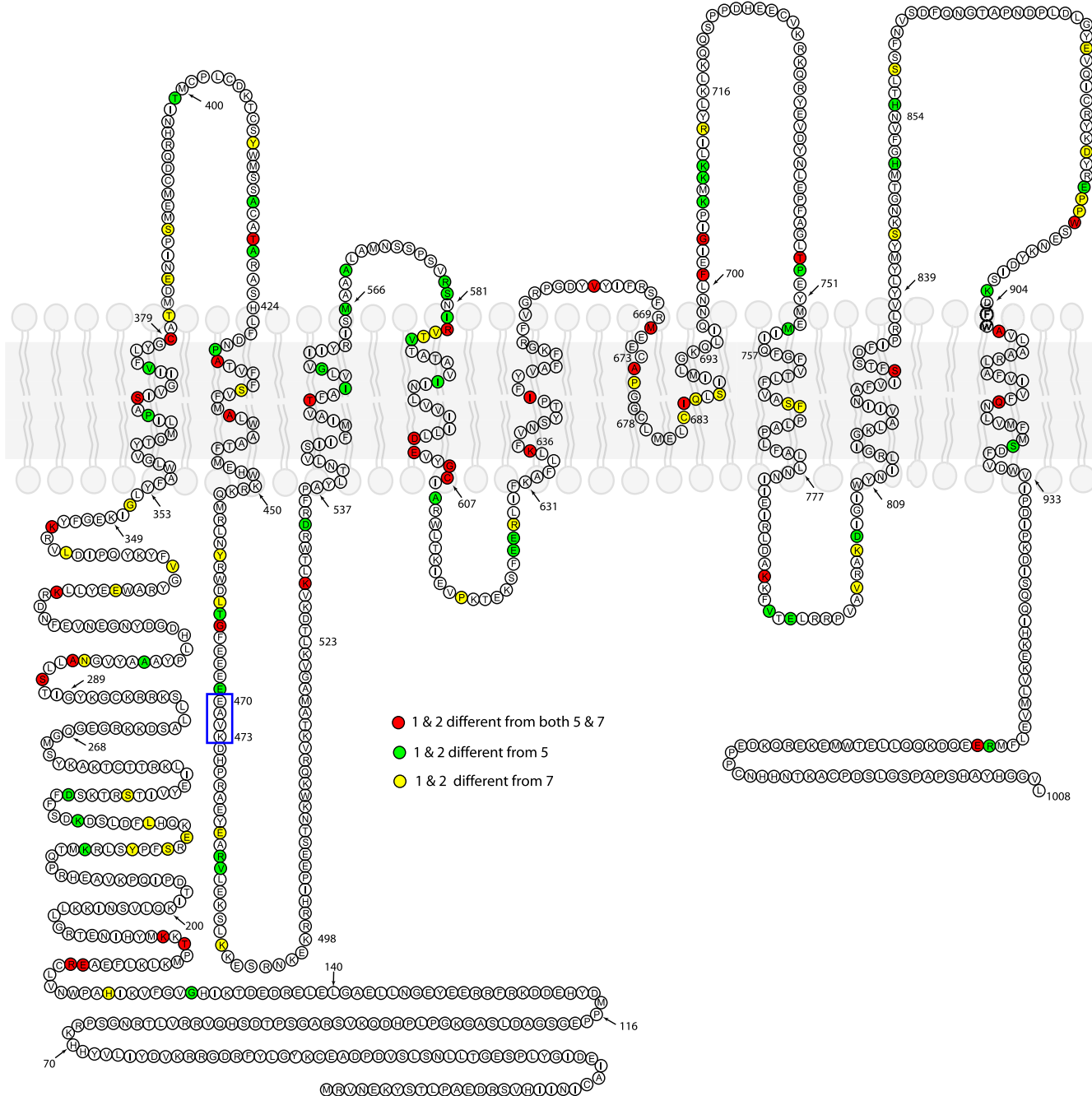


Fig. 6. Evolutionary divergence between ANO1 and 2 and ANO5 and 7. mANO1 sequence is shown. Available vertebrate ANO1, ANO2, ANO5, and ANO7 sequences were aligned and analyzed by DIVERGE 2.0 for type-II divergence to identify conserved amino acids of difference between ANO1/2 and ANO5/7. Amino acids colored red are amino acids that are conserved in both ANO1 and 2 that differ from conserved amino acids in both ANO5 and 7. Green: amino acids conserved in ANO1 and 2 that are different from conserved amino acids in ANO5 but not ANO7. Yellow: amino acids conserved in ANO1 and 2 that are different from conserved amino acids in ANO7 but not ANO5. Amino acids boxed in blue are unique to ANO1 and are critical for Ca^{2+} sensitivity, but are not conserved in ANO5 and ANO7.

first intracellular loop of mANO1 is important in determining the Ca^{2+} sensitivity of the channel (10, 41). In both ANO5 and ANO7, the EAVK sequence is not conserved. Therefore, we inserted EAVK after amino acid 462 to test whether the EAVK sequence was important in channel trafficking or activation. The ANO7 construct containing the EAVK sequence (chimera 7–1) did not produce current when expressed in HEK293 cells and did not traffic to the

plasma membrane (Fig. 7). Similar results were found with a chimera of ANO5 in which the entire first intracellular loop is composed of ANO1 sequence (chimera 5–1) (Fig. 8).

Because neither NH₂- and COOH-terminal sequences from ANO1 nor the EAVK sequence were sufficient to traffic ANO5 or ANO7 to the plasma membrane, we took a slightly different approach. We sought to determine whether the putative pore of ANO5 is functional when inserted into

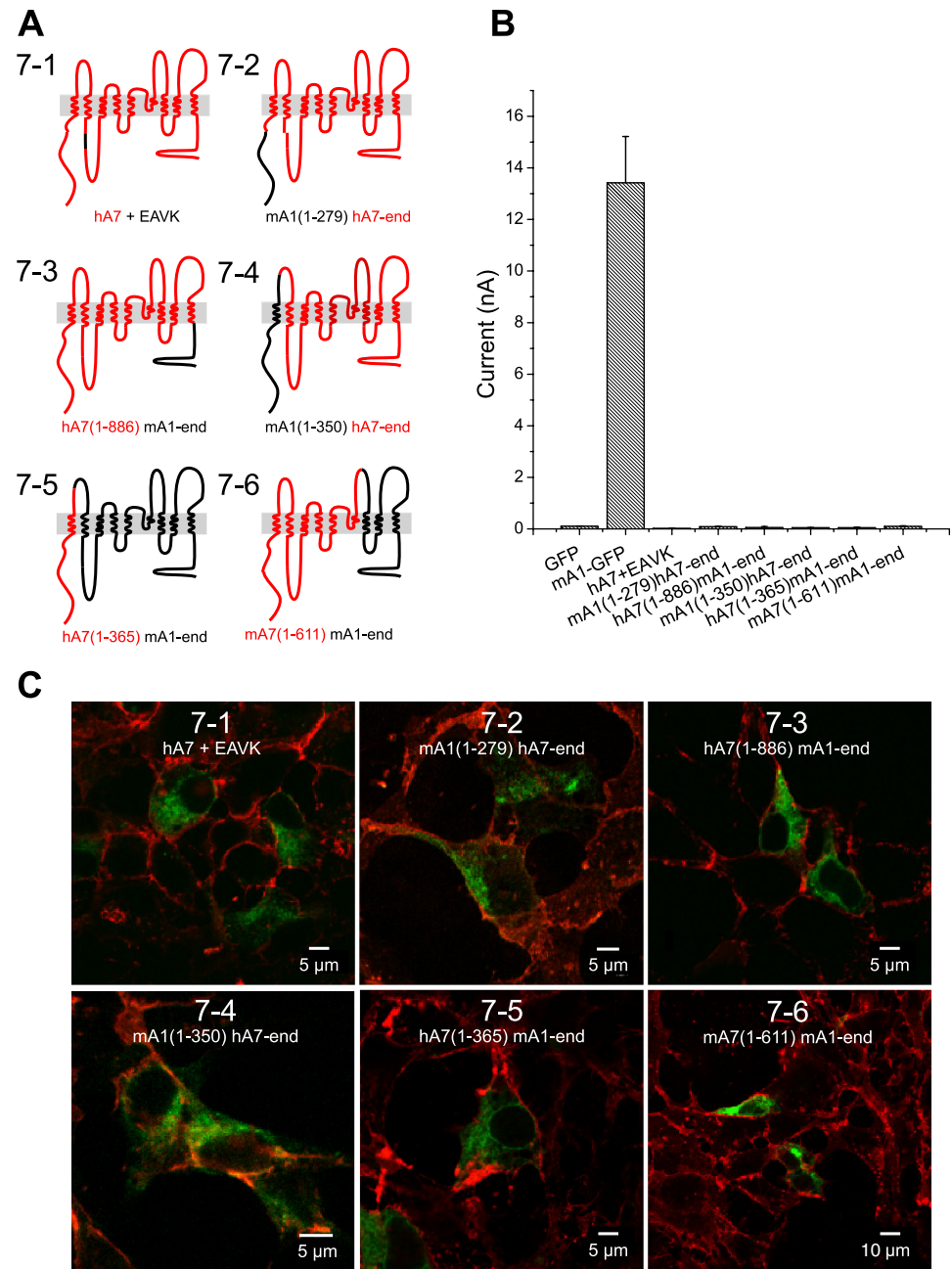


Fig. 7. Trafficking and Cl^- currents of chimeras between ANO1 and ANO7. *A*: cartoon of chimeric constructs. ANO1 (black), ANO5 (red). Chimeras are named based on the position of the residues included from either ANO1 (A1) or ANO7 (A7); for example, mA1(1-279)hA7-end includes the first 279 residues from ANO1 with the remaining residues belonging to ANO7. *B*: average current amplitudes of ANO1-ANO7 chimeras in transiently transfected HEK293 cells in response to 24 μM intracellular $[\text{Ca}^{2+}]$. *C*: confocal images showing localization of GFP-tagged ANO1-ANO7 chimeras counterstained with WGA.

ANO1. The reentrant loop between TM5 and TM6 in ANO1 is thought to form, at least in part, the conduction pathway of the channel (4, 42). If replacement of the ANO1 putative pore with that of ANO5 yields a functional channel, this would strongly suggest that ANO5 also functions as a CaCC. We initially replaced TM5 through TM6 of ANO1 with the corresponding sequence from ANO5 (chimera 5–3). This construct was not trafficked to the plasma membrane and did not generate current (Fig. 8). We then shortened the substituted ANO5 sequence to include only the putative reentrant loop (chimera 5–4). This chimera was also not trafficked to the plasma membrane and did not generate current. Surprisingly, Ano1 containing only 58 amino acids of ANO5 sequence in the reentrant loop (chimera 5–5) failed to be targeted to the plasma membrane or

to generate current. Likewise, ANO5 chimeras containing the ANO1 pore region (chimera 5–2) were intracellular (Fig. 8). These data suggest that the reentrant loop of ANO1 and ANO5 is sufficiently divergent, such that substitution of the ANO1 sequence with the corresponding sequence from ANO5 results in structurally aberrant protein. That none of the chimeras between ANO1 and ANO5/7 trafficked to the membrane indicates that ANOs 5 and 7 may have topologies that differ from ANO1.

DISCUSSION

Anoctamin family homology. Expression of ANO1 in several different cell types produces Ca^{2+} -activated Cl^- currents that resemble those of endogenous CaCCs. ANO2, which is

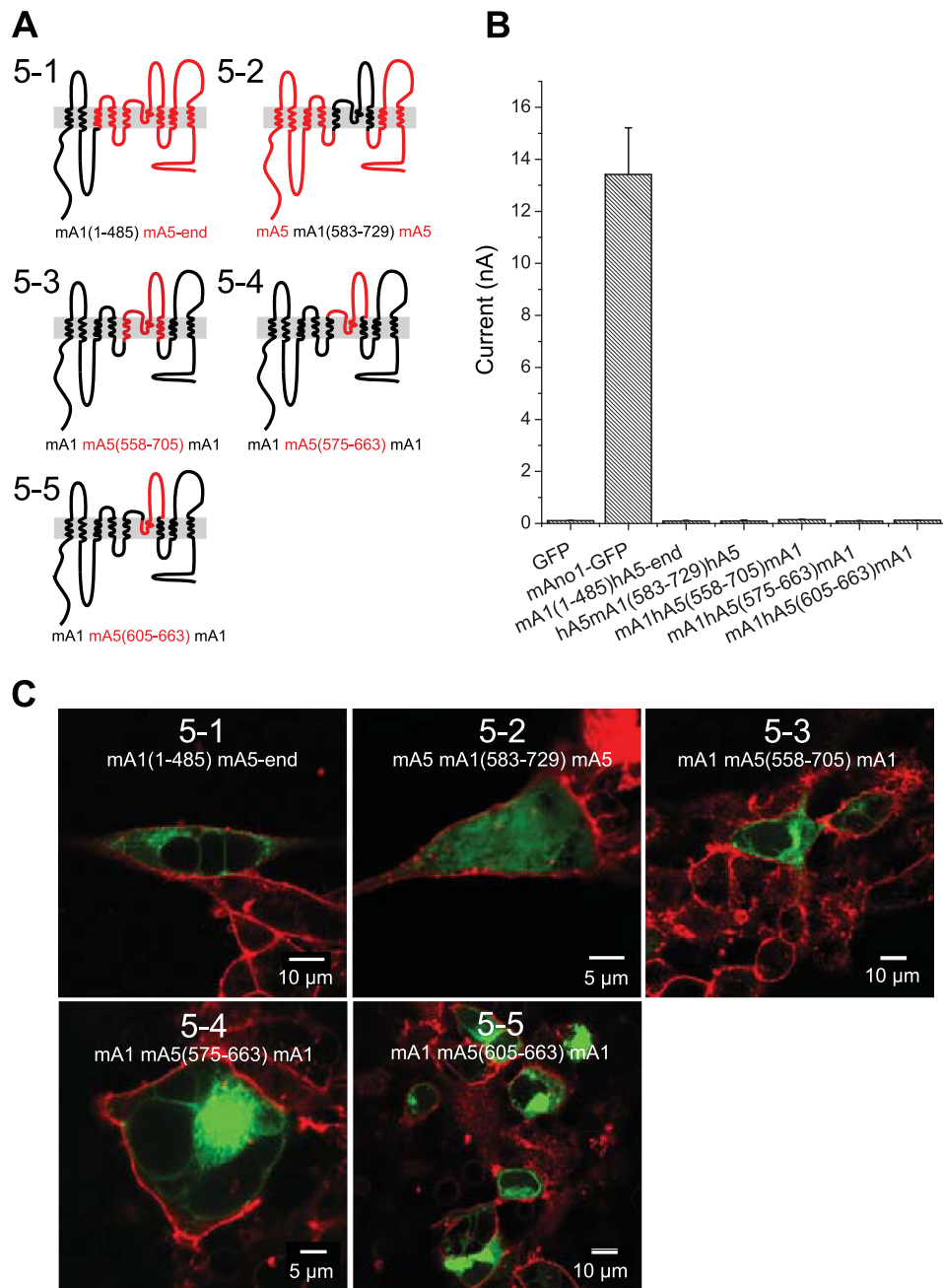


Fig. 8. Properties of ANO1-ANO5 chimeras. *A*: cartoon of ANO1-ANO5 chimeras. ANO1 (black). Ano5 (red). *B*: average current amplitudes of ANO1-ANO5 in transiently transfected HEK293 cells in response to 24 μ M intracellular $[Ca^{2+}]$. *C*: localization of GFP-tagged ANO1-ANO5 chimeras in transiently transfected HEK293 cells. Cells were counterstained with WGA.

\sim 57% identical in primary sequence to ANO1, has also been shown to produce Ca^{2+} -activated Cl^- currents. The conservation of sequence among the anoctamins suggests that other ANOs may also function as Cl^- channels. However, homology is not a certain predictor of protein function as shown by recent examples: certain voltage-gated Ca^{2+} channels in skeletal muscle are nonconductive to Ca^{2+} (33), the $\delta 2$ glutamate receptor is not activated by glutamate (19), and some of the ClC proteins are Cl^- channels and others are H^+-Cl^- exchangers (1). Although we have come to expect that similar sequence implies common function, it is clear that many structurally related proteins have different functions; for example, the *Escherichia coli* RecA protein, the bovine F1-ATPase, and *Salmonella typhimurium* adenosylcyclobinamide kinase all share the same highly conserved

core yet perform widely different functions of genetic recombination, ATP synthesis, and phosphorylation (8).

The topology of ANO7 has been studied using epitope tag insertion (6). The results of these experiments support an eight transmembrane topology model of ANO7 in which NH_2 - and $COOH$ -termini are cytoplasmic. The topology of other ANOs has not been explored experimentally, but it is thought that they are similar to ANO7 because of the primary amino acid sequence is highly conserved and the proteins exhibit very similar hydrophyt profiles. However, we have data that the topology of ANO1 is not as predicted in the region of the putative reentrant loop (Yu K, Duran C, Qu Z, Cui Y, Hartzell HC; unpublished observations). Small differences in sequence among the family members are likely to account for the differences in their trafficking and possibly also function.

The most notable difference between ANO1 and ANO5 or ANO7 is their localization. ANO1 is clearly expressed on the plasma membrane. However, ANOs 3–7 and ANO10 are intracellular in several expression systems as confirmed by whole cell patch clamp electrophysiology and confocal microscopy. We found that ANO7 colocalized with the ER marker mCherry-17 and displayed partial overlap with calnexin. However, ANO7 did not colocalize with markers for Golgi or endosomes in transfected cells. A search for ER retention signals within ANO5 and ANO7 revealed that neither contained the classical ER retention signal KDEL (24). However, ANO5 and ANO7 do have several RXR/KKXX potential retention signals that are not present in ANO1. These potential signals are mainly located in the NH₂-terminus, but replacement of the ANO5 or ANO7 NH₂-terminus with the ANO1 NH₂-terminus did not result in plasma membrane localization.

Further examination of the localization of ANO7 reveals that the majority of endogenous ANO7 in prostate is intracellular, but it remains unclear exactly in which subcellular structures it resides. We cannot rule out the possibility that some ANO7 is trafficked to the plasma membrane because we have not been able to identify a reliable apical membrane marker. Surprisingly, although the Na⁺-K⁺-ATPase has been reported to be apical in some studies (22) but not others (23), in our hands it is clearly basolateral in human prostate. Similarly, H⁺-K⁺-ATPase, which has been reported to be apical in mouse (27), is intracellular punctate in human. One possibility, although unlikely, is that the apical membrane has been destroyed during preparation of the tissue. Additional experiments are needed to refine the subcellular localization of endogenous ANO7, but our results indicate that ANO7 is primarily intracellular and is likely expressed in the ER. The fact that we find no current in transfected cells and no membrane localization in transfected cells or prostate, and that others have reported essentially background iodide fluxes in cells transfected with ANO7 (34), argues strongly that the primary function of ANO7 is not a plasma membrane Cl⁻ channel.

A similar situation exists with ANO5. Transient expression of ANO5 results in ER localization of the protein, but subcellular fractionation indicates that endogenous ANO5 resides in intracellular membrane vesicles (21, 40). Mizuta et al. (21) report that ANO5 resides predominantly in fractions that contain membranes from Golgi apparatus, secretory vesicles, endosomes, endoplasmic reticulum, and trans-Golgi network, and to a lesser degree in the plasma membrane fraction. However, the precise nature of the intracellular compartments in which it resides has not been determined (21).

ANO5 and ANO7 may have significant structural and functional differences from ANO1. We constructed several chimeras between ANO1 and ANO5 or 7 in an attempt to traffic ANO5 and ANO7 to the plasma membrane. However, relatively short sequences from ANO5 or 7 are sufficient to prevent ANO1 trafficking to the plasma membrane. Remarkably, replacement of a stretch of 59 amino acids within the predicted reentrant loop of ANO1 with corresponding sequences from ANO5 resulted in intracellular localization. This result is surprising in that the substituted region falls within a domain that is relatively well conserved across all members of the anoctamin family. The *anoctamin* domain, previously referred to as the DUF590 domain of unknown

function, is a COOH-terminal stretch of ~200 amino acids (Pfam PF04547). These data highlight the importance of this domain in anoctamin function and reveal notable differences between anoctamins in this region. One explanation of these results is that substitution of ANO1 sequences with sequences from ANO5 introduces targeting sequences that prevent trafficking to the plasma membrane. However, introduction of the corresponding ANO1 sequences to ANO5 did not result in functional plasma membrane channels. Similarly, chimeras between ANO1 and ANO7 were intracellular. These results demonstrate that ANO5 and ANO7 are significantly different, both structurally and functionally, from ANO1.

Are ANO5 and ANO7 CaCCs? Based on our findings, it is still unclear whether ANO5 and ANO7 are CaCCs. The intracellular localization of ANO 3–7 in several systems precludes the use of whole cell patch clamp electrophysiology to examine channel function. In a previous study by Schreiber et al. (34) it was suggested that ANO7 functioned as a CaCC. However, in iodide flux assays, the ATP- or ionomycin-stimulated flux carried by ANO7 was less than 10% as large as ANO1. Although a small fraction of ANO7 may traffic to the membrane, ANO7 is predominantly intracellular and generates currents indistinguishable from background. It is possible that anoctamins function as intracellular CaCCs.

It is possible that the iodide flux experiments are more sensitive than patch clamp, as it measures anion influx over a period of time. Nonetheless, it is surprising that the short form of ANO7 (ANO7S), which is a 179 amino acid protein with no predicted transmembrane domains, produced approximately the same iodide flux as the long form of ANO7. It is clear that Ano3–10 likely have roles in physiology distinct from that of ANO1 and may produce currents with properties very different from those of ANO1.

GRANTS

This study was supported by grants from the NIH GM-60448 (H. C. Hartzell) and EY014852 (H. C. Hartzell); Emory University Research Committee, the Microscopy Core of the Emory Neuroscience NINDS Core Facilities Grant P30NS055077; and NEI Core Grant P30EY006360. C. Duran was supported by training grant 5T32EY007092-25.

DISCLOSURES

No conflicts of interest, financial or otherwise, are declared by the author(s).

AUTHOR CONTRIBUTIONS

Author contributions: C.D., Z.Q., and H.C.H. conception and design of research; C.D., Z.Q., Y.C., and H.C.H. performed experiments; C.D., Z.Q., and Y.C. analyzed data; C.D., Z.Q., A.O.O., and H.C.H. interpreted results of experiments; C.D. prepared figures; C.D. drafted manuscript; C.D., Z.Q., A.O.O., and H.C.H. edited and revised manuscript; C.D., Z.Q., A.O.O., and H.C.H. approved final version of manuscript.

REFERENCES

- Accardi A, Picollo A. CLC channels and transporters: proteins with borderline personalities. *Biochim Biophys Acta* 1798: 1457–1464, 2010.
- Bolduc V, Marlow G, Boycott KM, Saleki K, Inoue H, Kroon J, Itakura M, Robitaille Y, Parent L, Baas F, Mizuta K, Kamata N, Richard I, Linssen WH, Mahjneh I, de Visser M, Bashir R, Brais B. Recessive mutations in the putative calcium-activated chloride channel Anoctamin 5 cause proximal LGMD2L and distal MMD3 muscular dystrophies. *Am J Hum Genet* 86: 213–221, 2010.

3. Brambillasca S, Yabal M, Makarow M, Borgese N. Unassisted translocation of large polypeptide domains across phospholipid bilayers. *J Cell Biol* 175: 767–777, 2006.
4. Caputo A, Caci E, Ferrera L, Pedemonte N, Barsanti C, Sondo E, Pfeffer U, Ravazzolo R, Zegarra-Moran O, Galietta LJ. TMEM16A, a membrane protein associated with calcium-dependent chloride channel activity. *Science* 322: 590–594, 2008.
5. Das S, Hahn Y, Nagata S, Willingham MC, Bera TK, Lee B, Pastan I. NGEP, a prostate-specific plasma membrane protein that promotes the association of LNCaP cells. *Cancer Res* 67: 1594–1601, 2007.
6. Das S, Hahn Y, Walker DA, Nagata S, Willingham MC, Peehl DM, Bera TK, Lee B, Pastan I. Topology of NGEP, a prostate-specific cell:cell junction protein widely expressed in many cancers of different grade level. *Cancer Res* 68: 6306–6312, 2008.
7. Dutta AK, Khimji AK, Kresge C, Bugde A, Dougherty M, Esser V, Ueno Y, Glaser SS, Alpini G, Rockey DC, Feranchak AP. Identification and functional characterization of TMEM16A, a Ca^{2+} -activated Cl^- channel activated by extracellular nucleotides, in biliary epithelium. *J Biol Chem* 286: 766–776, 2011.
8. Egelman EH. Reducing irreducible complexity: divergence of quaternary structure and function in macromolecular assemblies. *Curr Opin Cell Biol* 22: 68–74, 2010.
9. Eggemont J. Calcium-activated chloride channels: (un)known, (un)loved? *Proc Am Thorac Soc* 1: 22–27, 2004.
10. Ferrera L, Caputo A, Ubby I, Bussani E, Zegarra-Moran O, Ravazzolo R, Pagani F, Galietta LJ. Regulation of TMEM16A chloride channel properties by alternative splicing. *J Biol Chem* 284: 33360–33368, 2009.
11. Hartzell HC, Yu K, Xiao Q, Chien LT, Qu Z. Anoctamin/TMEM16 family members are Ca^{2+} -activated Cl^- channels. *J Physiol* 587: 2127–2139, 2009.
12. Hicks D, Sarkozy A, Muelas N, Koehler K, Huebner A, Hudson G, Chinnery PF, Barresi R, Eagle M, Polvikoski T, Bailey G, Miller J, Radunovic A, Hughes PJ, Roberts R, Krause S, Walter MC, Laval SH, Straub V, Lochmuller H, Bushby K. A founder mutation in Anoctamin 5 is a major cause of limb-girdle muscular dystrophy. *Brain* 134: 171–182, 2011.
13. Horton RM, Hunt HD, Ho SN, Pullen JK, Pease LR. Engineering hybrid genes without the use of restriction enzymes: gene splicing by overlap extension. *Gene* 77: 61–68, 1989.
14. Huang F, Rock JR, Harfe BD, Cheng T, Huang X, Jan YN, Jan LY. Studies on expression and function of the TMEM16A calcium-activated chloride channel. *Proc Natl Acad Sci USA* 106: 21413–21418, 2009.
15. Kiessling A, Weigle B, Fuessel S, Ebner R, Meye A, Rieger MA, Schmitz M, Temme A, Bachmann M, Wirth MP, Rieber EP. D-TMPP: a novel androgen-regulated gene preferentially expressed in prostate and prostate cancer that is the first characterized member of an eukaryotic gene family. *Prostate* 64: 387–400, 2005.
16. Kuruma A, Hartzell HC. Bimodal control of a $\text{Ca}(2+)$ -activated Cl^- channel by different $\text{Ca}(2+)$ signals. *J Gen Physiol* 115: 59–80, 2000.
17. Mahjneh I, Jaiswal J, Lamminen A, Somer M, Marlow G, Kiuru-Enari S, Bashir R. A new distal myopathy with mutation in anoctamin 5. *Neuromuscul Disord* 20: 791–795, 2010.
18. Manoury B, Tamulevičiute A, Tammaro P. TMEM16A/anoctamin 1 protein mediates calcium-activated chloride currents in pulmonary arterial smooth muscle cells. *J Physiol* 588: 2305–2314, 2010.
19. Matsuda K, Miura E, Miyazaki T, Kakegawa W, Emi K, Narumi S, Fukazawa Y, Ito-Ishida A, Kondo T, Shigemoto R, Watanabe M, Yuzaki M. Cbln1 is a ligand for an orphan glutamate receptor delta2, a bidirectional synapse organizer. *Science* 328: 363–368, 2010.
20. Milenkovic VM, Brockmann M, Stohr H, Weber BH, Strauss O. Evolution and functional divergence of the anoctamin family of membrane proteins. *BMC Evol Biol* 10: 319, 2010.
21. Mizuta K, Tsutsumi S, Inoue H, Sakamoto Y, Miyatake K, Miyawaki K, Noji S, Kamata N, Itakura M. Molecular characterization of GDD1/TMEM16E, the gene product responsible for autosomal dominant gnathodiaphyseal dysplasia. *Biochem Biophys Res Commun* 357: 126–132, 2007.
22. Mobasheri A, Oukrif D, Dawodu SP, Sinha M, Greenwell P, Stewart D, Djamgoz MB, Foster CS, Martin-Vasallo P, Mobasheri R. Isoforms of Na^+ , K^+ -ATPase in human prostate; specificity of expression and apical membrane polarization. *Histol Histopathol* 16: 141–154, 2001.
23. Mobasheri A, Pestov NB, Papanicolaou S, Kajee R, Cozar-Castellano I, Avila J, Martin-Vasallo P, Foster CS, Modyanov NN, Djamgoz MB. Expression and cellular localization of Na,K -ATPase isoforms in the rat ventral prostate. *BJU Int* 92: 793–802, 2003.
24. Munro S, Pelham HR. A C-terminal signal prevents secretion of luminal ER proteins. *Cell* 48: 899–907, 1987.
25. Namkung W, Phuan PW, Verkman AS. TMEM16A inhibitors reveal TMEM16A as a minor component of CaCC conductance in airway and intestinal epithelial cells. *J Biol Chem* 286: 2365–2374, 2011.
26. Ousingsawat J, Martins JR, Schreiber R, Rock JR, Harfe BD, Kunzelmann K. Loss of TMEM16A causes a defect in epithelial Ca^{2+} -dependent chloride transport. *J Biol Chem* 284: 28698–28703, 2009.
27. Pestov NB, Korneenko TV, Adams G, Tillekeratne M, Shakharonov MI, Modyanov NN. Nongastric H-K-ATPase in rodent prostate: lobe-specific expression and apical localization. *Am J Physiol Cell Physiol* 282: C907–C916, 2002.
28. Pifferi S, Dibattista M, Menini A. TMEM16B induces chloride currents activated by calcium in mammalian cells. *Pflügers Arch* 458: 1023–1038, 2009.
29. Rasche S, Toetter B, Adler J, Tschapek A, Doerner JF, Kurtenbach S, Hatt H, Meyer H, Warscheid B, Neuhaus EM. Tmem16b is specifically expressed in the cilia of olfactory sensory neurons. *Chem Senses* 35: 239–245, 2010.
30. Romanenko VG, Catalan MA, Brown DA, Putzier I, Hartzell HC, Marmorstein AD, Gonzalez-Begne M, Rock JR, Harfe BD, Melvin JE. Tmem16A encodes the Ca^{2+} -activated Cl^- channel in mouse submandibular salivary gland acinar cells. *J Biol Chem* 285: 12990–13001, 2010.
31. Ronchi P, Colombo S, Francolini M, Borgese N. Transmembrane domain-dependent partitioning of membrane proteins within the endoplasmic reticulum. *J Cell Biol* 181: 105–118, 2008.
32. Sagheddu C, Boccaccio A, Dibattista M, Montani G, Tirindelli R, Menini A. Calcium concentration jumps reveal dynamic ion selectivity of calcium-activated chloride currents in mouse olfactory sensory neurons and TMEM16b-transfected HEK 293T cells. *J Physiol* 588: 4189–4204, 2010.
33. Schredelseker J, Shrivastav M, Dayal A, Grabner M. Non- Ca^{2+} -conducting Ca^{2+} channels in fish skeletal muscle excitation-contraction coupling. *Proc Natl Acad Sci USA* 107: 5658–5663, 2010.
34. Schreiber R, Uliyakina I, Kongsuphol P, Warth R, Mirza M, Martins JR, Kunzelmann K. Expression and function of epithelial anoctamins. *J Biol Chem* 285: 7838–7845, 2010.
35. Schroeder BC, Cheng T, Jan YN, Jan LY. Expression cloning of TMEM16A as a calcium-activated chloride channel subunit. *Cell* 134: 1019–1029, 2008.
36. Shen H, Chou JJ. MemBrain: improving the accuracy of predicting transmembrane helices. *PLoS One* 3: e2399, 2008.
37. Stephan AB, Shum EY, Hirsh S, Cygnar KD, Reisert J, Zhao H. ANO2 is the ciliary calcium-activated chloride channel that may mediate olfactory amplification. *Proc Natl Acad Sci USA* 106: 11776–11781, 2009.
38. Stohr H, Heisig JB, Benz PM, Schoberl S, Milenkovic VM, Strauss O, Aartsen WM, Wijnholds J, Weber BH, Schulz HL. TMEM16B, a novel protein with calcium-dependent chloride channel activity, associates with a presynaptic protein complex in photoreceptor terminals. *J Neurosci* 29: 6809–6818, 2009.
39. Tsutsumi S, Inoue H, Sakamoto Y, Mizuta K, Kamata N, Itakura M. Molecular cloning and characterization of the murine gnathodiaphyseal dysplasia gene GDD1. *Biochem Biophys Res Commun* 331: 1099–1106, 2005.
40. Tsutsumi S, Kamata N, Vokes TJ, Maruoka Y, Nakakuki K, Enomoto S, Omura K, Amagasa T, Nagayama M, Saito-Ohara F, Inazawa J, Moritani M, Yamaoka T, Inoue H, Itakura M. The novel gene encoding a putative transmembrane protein is mutated in gnathodiaphyseal dysplasia (GDD). *Am J Hum Genet* 74: 1255–1261, 2004.
41. Xiao Q, Yu K, Perez-Cornejo P, Cui Y, Arreola J, Hartzell HC. Voltage- and calcium-dependent gating of TMEM16A/Ano1 chloride channels are physically coupled by the first intracellular loop. *Proc Natl Acad Sci USA* 108: 8891–8896, 2011.
42. Yang YD, Cho H, Koo JY, Tak MH, Cho Y, Shim WS, Park SP, Lee J, Lee B, Kim BM, Raouf R, Shin YK, Oh U. TMEM16A confers receptor-activated calcium-dependent chloride conductance. *Nature* 455: 1210–1215, 2008.